DISEASES AND DISORDERS

Disruption in *ACTL7A* causes acrosomal ultrastructural defects in human and mouse sperm as a novel male factor inducing early embryonic arrest

Aijie Xin[1,2]*, Ronggui Qu[1]*, Guowu Chen[1]*, Ling Zhang[1,3,4]*, Junling Chen[1], Chengqiu Tao[3], Jing Fu[1], Jianan Tang[2], Yanfei Ru[2], Ying Chen[1], Xiandong Peng[1], Huijuan Shi[2†], Feng Zhang[1,2,3,4,5†], Xiaoxi Sun[1,4,6†]

Early embryonic arrest is a challenge for in vitro fertilization (IVF). No genetic factors were previously revealed in the sperm-derived arrest of embryonic development. Here, we reported two infertile brothers presenting normal in conventional semen analysis, but both couples had no embryos for transfer after several IVF and intracytoplasmic sperm injection (ICSI). Whole-exome sequencing identified a homozygous missense mutation of *ACTL7A* in both brothers. This mutation is deleterious and causes sperm acrosomal ultrastructural defects. The *Actl7a* knock-in mouse model was generated, and male mutated mice showed sperm acrosomal defects, which were completely consistent with the observations in patients. Furthermore, the sperm from *ACTL7A*/*Actl7a*-mutated men and mice showed reduced expression and abnormal localization of PLCζ as a potential cause of embryonic arrest and failure of fertilization. Artificial oocyte activation could successfully overcome the *Actl7a*-mutated sperm-derived infertility, which is meaningful in the future practice of IVF/ICSI for the *ACTL7A*-associated male infertility.

INTRODUCTION

In mammals, fertilization is the process in which a capacitated spermatozoon fuses with the oocyte, subsequently initiating the development of an embryo, i.e., a new individual. Naturally, this process occurs within the fallopian tube. Assisted reproductive technologies (ARTs), including in vitro fertilization (IVF) and intracytoplasmic sperm injection (ICSI), enable the fertilization of the oocyte and sperm, and subsequently, the development of viable embryos in vitro. ARTs have helped millions of infertile couples to have their own offspring. However, for unexplained infertile couples who suffer from recurrent early embryonic arrest, especially with seemingly "normal" sperm and oocytes, it is challenging for clinicians to diagnose and formulate a reasonable treatment. In general, the clinicians attribute it to female factors rather than male ones, especially when sperm has been clinically diagnosed as normal. Although two maternal effect genes, *TLE6* and *WEE2*, have been reported to be associated with the failure of early embryonic development (*1*, *2*), there have been no reports regarding male genetic factors leading to the failure of early embryonic development in humans.

In this study, we found a novel homozygous mutation of *ACTL7A* in a consanguineous family with two affected brothers causing the early embryonic arrest and confirmed the sperm-derived infertility by construction of *Actl7a* knock-in mouse model corresponding to the human mutation. Transmission electron microscopy (TEM) in sperm of the affected brothers and the mouse model revealed the consistent acrosomal ultrastructural defects, which were beyond the resolution of light microscopy of conventional semen analysis. Therefore, the *ACTL7A*-associated male infertility cannot be readily diagnosed in the clinic. Instead, the genetic test based on *ACTL7A* can be an efficient method to identify this previously neglected male factor for early embryonic arrest. Artificial oocyte activation (AOA) could successfully overcome the embryonic arrest and make the *Actl7a* mutation mice have offspring. This study is the first report that a homozygous *ACTL7A* mutation leads to sperm-derived early embryonic arrest and AOA could be a potential therapeutic treatment for the *ACTL7A*-mutated male infertility in humans.

RESULTS

A male factor causes human early embryonic arrest

Here, we found two couples with unexplained infertility from a consanguineous family (Fig. 1A). The two brothers had no previous records of substantial illnesses, and the complete andrological examinations revealed normal results. In addition, both of them were clinically shown to have normal sperm morphology under light microscopy (fig. S1) and well semen parameters above the lower reference limits stated in the fifth edition of the World Health Organization (WHO) laboratory manual (table S1). However, during the IVF procedure, the sperms from both the brothers could not fertilize the oocytes from their respective wives. Following ICSI, several oocytes developed into embryos, but they arrested at the four-cell or five-cell stage (fig. S2). In total, 51 MII oocytes from the two brothers' wives were used for IVF or ICSI, but no embryos were suitable for transfer (table S2). However, both couples eventually had healthy babies following IVF with donated sperms (table S2). These clinical observations excluded female factors and suggested that a male factor may lead to the failure of early embryonic development and infertility.

[1]Shanghai Ji Ai Genetics and IVF Institute, Obstetrics and Gynecology Hospital, Fudan University, Shanghai, China. [2]NHC Key Laboratory of Reproduction Regulation (Shanghai Institute of Planned Parenthood Research), School of Pharmacy, Fudan University, Shanghai, China. [3]State Key Laboratory of Genetic Engineering, School of Life Sciences, Fudan University, Shanghai, China. [4]Shanghai Key Laboratory of Female Reproductive Endocrine Related Diseases, Shanghai, China. [5]State Key Laboratory of Reproductive Medicine, Center for Global Health, School of Public Health, Nanjing Medical University, Nanjing, China. [6]Department of Endocrinology and Reproductive Medicine, Obstetrics and Gynecology Hospital, Fudan University, Shanghai, China.
*These authors contributed equally to this work.
†Corresponding author. Email: xiaoxi_sun@aliyun.com (X.S.); zhangfeng@fudan.edu.cn (F.Z.); shihuijuan2011@163.com (H.S.)

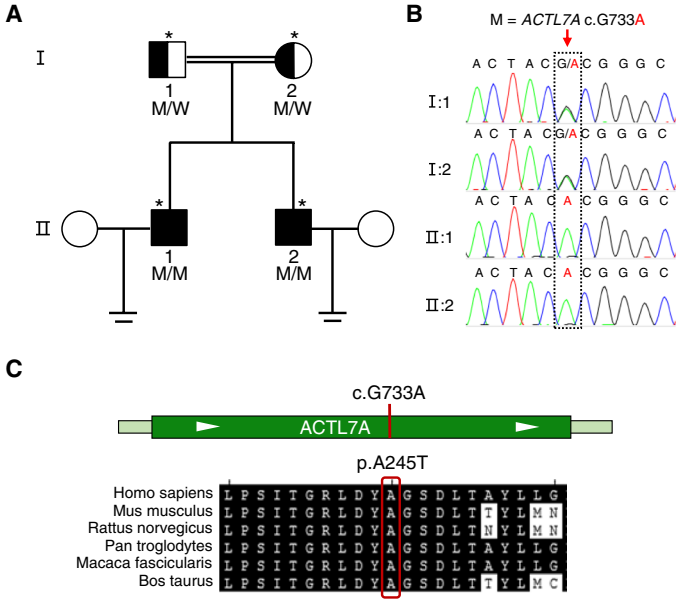

Fig. 1. Identification of a homozygous *ACTL7A* mutation in two brothers with infertility. (**A**) Pedigree of a family with an inherited *ACTL7A* mutation. The open square and circles denoted the unaffected male and female family members, respectively. The filled squares denote the affected male members, and the double line indicates a consanguineous marriage. Individuals marked with an asterisk were investigated by WES. M, mutation; W, wild type. (**B**) The *ACTL7A* mutation was verified by Sanger sequencing. The homozygous *ACTL7A* mutation of both brothers (subjects II:1 and II:2) was inherited from heterozygous parental carriers (subjects I:1 and I:2). The dotted rectangle indicates the position of the mutation. (**C**) Location and conservation of the *ACTL7A* mutation. The conservation of the mutated amino acid is indicated by the alignment of this sequence with that of six mammalian species.

Table 1. Homozygous *ACTL7A* mutation identified in two brothers affected by male infertility.

	Brothers 1 and 2
Gene	*ACTL7A*
Variant coordinates*	Chr9:111625335, G>A
Transcript	NM_006687
cDNA mutation	c.733G>A
Protein alteration	p.Ala245Thr
Mutation type	Missense, homozygous
Allele frequencies in human populations	
Allele frequency in gnomAD	4.068×10^{-6}
Number of homozygotes	0
Conservation†	
Phastcons	1
Phylop	4.084
Functional prediction	
PROVEAN	Deleterious
PolyPhen-2	Probably damaging
MutationTaster	Disease causing

*Variant coordinate is based on the human genome assembly GRCh37/h19.
†The Phastcons value is close to 1 when a nucleotide is conserved, and the predicted conserved sites are assigned positive scores by Phylop.

WES identified a novel homozygous mutation of *ACTL7A* in both affected brothers

To investigate the unknown male factor responsible for early embryonic arrest, we performed whole-exome sequencing (WES) of the two brothers and their parents. A previously unidentified homozygous mutation of *ACTL7A* was identified in both brothers (subjects II-1 and II-2 in Fig. 1, A and B). This missense mutation c.733G>A (p. Ala245Thr) of *ACTL7A* was confirmed to be inherited from heterozygous parental carriers by Sanger sequencing (Fig. 1, A and B). The allele frequency of *ACTL7A* c.733G>A in human populations was extremely low (4.068×10^{-6}), and its homozygote was absent in 141,456 individuals in the Genome Aggregation Database (gnomAD database) (Table 1). This evidence is consistent with our contention that this rare missense mutation of *ACTL7A* might be pathogenic and under purifying selection. In addition, this mutation located at a highly conserved position of *ACTL7A* (Fig. 1C) and showed evolutionary conservation, as indicated by two methods (PhastCons and PhyloP; Table 1). It was predicted to be potentially deleterious by all three bioinformatic predictors (PolyPhen-2, PROVEAN, and MutationTaster) (Table 1).

Disruption in ACTL7A led to acrosomal ultrastructural defects

It has been reported that ACTL7A is localized on the acrosome in mouse sperms (*3*). Therefore, we analyzed the localization of human ACTL7A in the sperm of affected brothers by immunofluorescence assays. As shown in Fig. 2A, in case of the normal control, the signals of ACTL7A overlapped almost completely with those of the sperm outer acrosomal membrane marker peanut agglutinin (PNA). However, ACTL7A signals were absent in case of the brothers' spermatozoa. In addition, we found that the PNA signals presented nonuniform distribution in patients' spermatozoa. Furthermore, we investigated the acrosomal matrix using acrosin, a major proteinase present in the acrosome of mature spermatozoa, and revealed that acrosin signals were also distributed unevenly (Fig. 2B). To further explore the acrosomal abnormalities, we analyzed the ultrastructures of the spermatozoa from both affected brothers by TEM. Compared with the spermatozoa of the healthy male control, the sperm acrosome of the *ACTL7A*-mutated brother demonstrated detachment from the nuclear envelope and showed a shedding and folding form (Fig. 2C). These experimental observations indicated that the homozygous *ACTL7A* mutation could lead to acrosomal defects in human sperms.

Homozygous *Actl7a* knock-in mutation causes failure of proacrosomal vesicle fusion in mice

The knock-in mutation in the mouse ortholog *Actl7a* was induced by the CRISPR-Cas9 technology. The guanine at the 748th position of the *Actl7a*-coding region was mutated to adenine, which altered the codon from GCA to ACA, leading to the conversion of the amino acid glycine to threonine (Fig. 3A). The real-time quantitative polymerase chain reaction (PCR) analysis showed that the relative mRNA levels of *Actl7a* in the testes of the *Actl7a*-mutated mice ($Actl7a^{KI/KI}$) decreased significantly (by approximately 30%) when

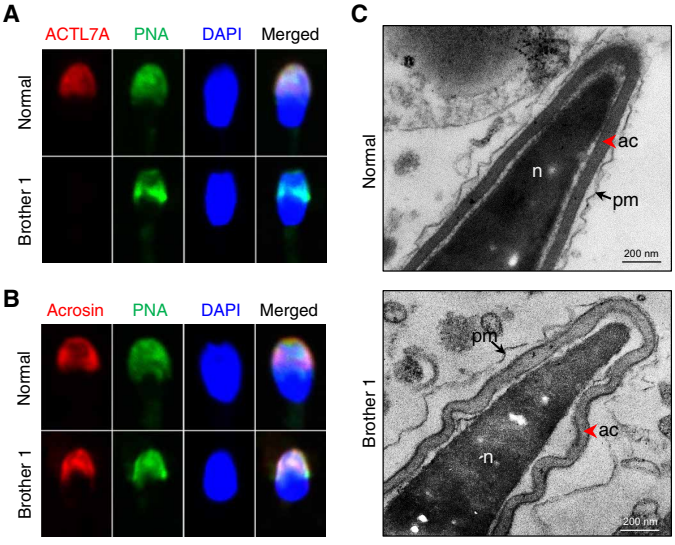

Fig. 2. Homozygous mutation in *ACTL7A* caused the ultrastructural impairment of sperm acrosomes in the two infertile brothers. (**A**) The signal of ACTL7A disappeared in the case of the spermatozoa from the infertile brothers carrying the homozygous *ACTL7A* mutation. The localization of ACTL7A was identified using polyclonal antibodies against ACTL7A, followed by the secondary antibodies (donkey anti-rabbit–Cy3; red). The acrosome and sperm nuclei were stained with PNA (green) and DAPI (blue), respectively. Scale bars, 2 μm. (**B**) The acrosome signals were distributed nonuniformly in sperm of brother 1. Acrosin (red) was a marker of acrosomal matrix. PNA (green) labels the outer acrosomal membrane. (**C**) The ultrastructure of sperms from the brothers with the *ACTL7A* mutation revealed acrosome detachment. The red arrowhead indicates the acrosome. The arrow indicates the plasma membrane. ac, acrosome; n, nucleus; pm, plasma membrane. Scale bars, 200 nm. Photo credit: Aijie Xin, Fudan University.

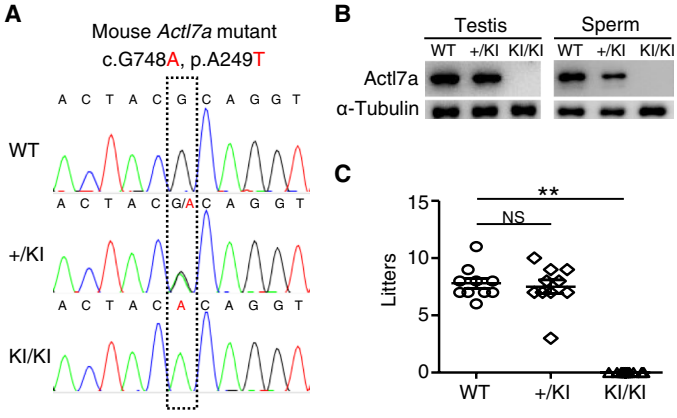

Fig. 3. Homozygous knock-in mutation in *Actl7a* leads to male infertility in the mouse model. (**A**) Genotyping of the constructed *Actl7a* knock-in (KI) mutation in mice. WT, wild type; +/KI, heterozygous mutation; KI/KI, homozygous mutation. (**B**) The ACTL7A protein was completely absent in the testes and sperms of *Actl7a*$^{KI/KI}$ mice. α-Tubulin was used as a loading control. (**C**) The *Actl7a*$^{KI/KI}$ male mice were completely infertile. The fertility assessment experiments were performed for the male WT (WT; $n = 5$) mice and the male mice with heterozygous (+/KI; $n = 5$) and homozygous (KI/KI; $n = 5$) mutations. One-way ANOVA, $^{**}P < 0.01$; NS, not significant. Data are means ± SEM.

compared with that in the wild type (WT) (fig. S3). This mutation led to the complete absence of the ACTL7A protein in both testes and sperms of the *Actl7a*$^{KI/KI}$ male mice, indicating that this missense mutation is a loss-of-function mutation (Fig. 3B). The ubiquitin-proteasome pathway, a major mechanism for the targeted degradation of unstable proteins in eukaryotic cells (*4*), may be involved in the degradation of the ACTL7A mutant protein, leading to the loss of this protein in *Actl7a*$^{KI/KI}$ mice.

To investigate the infertility of *Actl7a*$^{KI/KI}$ mice, both male and female mice with the *Actl7a* knock-in mutation were mated with the WT mice. We found that the *Actl7a*$^{KI/KI}$ male mice were infertile (Fig. 3C), whereas the *Actl7a*$^{KI/KI}$ female mice could generate offspring and presented no obvious defects in fertility. The semen characteristics, testis size, or weight demonstrated no significant differences between the WT and *Actl7a*$^{KI/KI}$ male mice (fig. S4, A to C). Histological examination of the testicular and epididymis sections stained with hematoxylin and eosin indicated a normal spermatogenesis process; the seminiferous tubules and epididymis were not affected by the homozygous *Actl7a* mutation in mice (fig. S4D).

Because no commercial antibodies against mouse ACTL7A were available for immunofluorescence, we detected the integrity of the sperm acrosomes by PNA and acrosin. Similar to the case for the brothers carrying homozygous *ACTL7A* mutation, the signals of both acrosome markers were distributed nonuniformly in the spermatozoa of the *Actl7a*$^{KI/KI}$ mice (Fig. 4A). Furthermore, the acrosomal morphology changed from the sickle shape in WT mice to the cap-like structure in *Actl7a*$^{KI/KI}$ mice (Fig. 4A). TEM observations of the spermatozoa from *Actl7a*$^{KI/KI}$ male mice were also consistent with those of the spermatozoa from the two brothers, presenting the detachment of the acrosome from the nuclear envelope of the sperm (Fig. 4B). On the basis of the above analyses, the phenotypes of *Actl7a*-mutated male mice were identical to those of the two brothers. These data confirmed that the *Actl7a* knock-in mutation led to male infertility via acrosomal defects.

To further investigate the mechanism of this mutation causing sperm acrosomal defects, we characterized the structural details of spermatids during acrosome biogenesis in WT and *Actl7a*$^{KI/KI}$ mice by TEM. In normal conditions, numerous small Golgi-derived proacrosomic vesicles are transported to the nuclear surface (Golgi phase; Fig. 4C, a and a′). The vesicles gradually fuse and attach to the nuclear envelope through the acroplaxome forming an acrosomal cap (cap phase; Fig. 4C, b and b′). The acrosomal cap further develops and flattens over half of the nucleus in acrosomal phase (Fig. 4C, c and c′), and the acrosome structure is completed at the end of maturation phase (Fig. 4C, d and d′). However, the acrosomes developed abnormally in the male *Actl7a*$^{KI/KI}$ mice. In the first stage, it presented big and atypical proacrosomic vesicles during Golgi phase (Fig. 4C, e and e′). Then, they fail to fuse with the acrosome (Fig. 4C, f and f′) and gradually accumulate, eventually causing the abnormal acrosome detached from the nuclear envelope (Fig. 4C, g, g′, h, and h′). Although it has been reported that ACTL7A is located on the subacrosomal layer, known as the acroplaxome (*3*), the results of TEM demonstrated normal acroplaxome structures in testis of *Actl7a*$^{KI/KI}$ mice. These experimental observations suggested that ACTL7A might not be involved in acroplaxome assembly but played an important role in formation and fusion of Golgi-derived vesicles during acrosome biogenesis.

Abnormal localization of PLCζ in sperm from *Actl7a*-mutated mice and overcoming its associated embryonic arrest by AOA

Considering the failure of ART in case of the two brothers in the clinic, we performed IVF/ICSI using the sperms of *Actl7a*-mutated

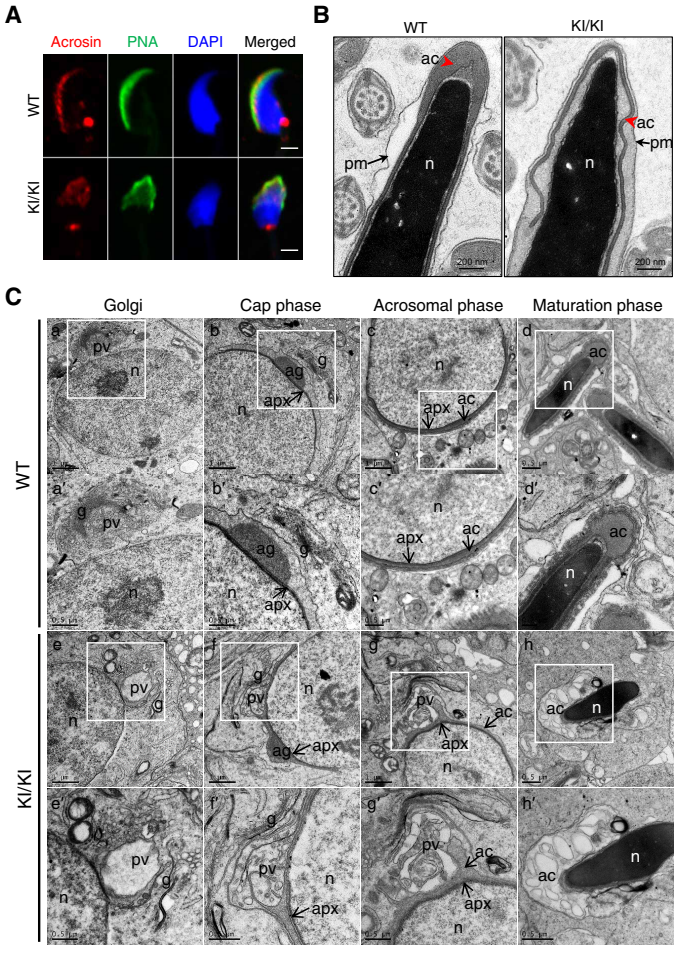

Fig. 4. Homozygous knock-in mutation in mouse *Actl7a* causes acrosomal defects due to fusion failure of proacrosomal vesicle. (**A**) The location of acrosome changed in sperm from the *Actl7a*$^{KI/KI}$ mice. Acrosin (red) and PNA represented acrosomal matrix and the outer acrosomal membrane, respectively. Sperm nuclei were stained with DAPI (blue). Scale bars, 2 μm. (**B**) TEM analysis revealed the detachment of the acrosome (ac) from the sperm nuclei (n) in the sperms from the *Actl7a*$^{KI/KI}$ mice. The red arrowhead indicates the acrosome. The arrow indicates the plasma membrane (pm). (**C**) Acrosome biogenesis of WT and *Actl7a*$^{KI/KI}$ mouse spermatid. (a to d) Four phases of acrosome biogenesis in WT. Golgi phase (a), cap phase (b), acrosomal phase (c), and maturation phase (d). (a′ to d′) Higher magnification of the boxed region from (a) to (b). Numerous proacrosomal vesicles derived from the trans-face of the Golgi (a and a′) attached to the acroplaxome forming a cap over the nucleus (b and b′). Acrosome further developed and flattened over half of the nucleus in acrosomal phase (c and c′) and continued to maturation (d and d′). (e to e′) Four corresponding phases in *Actl7a*$^{KI/KI}$ mouse. (e′ to h′) Higher magnification of the boxed region from (e) to (h). Big and atypical proacrosomic vesicles generated during Golgi phase (e and e′). The proacrosomal vesicle fusion failed (f and f′) and accumulated gradually (g and g′), eventually causing the abnormal acrosome detached from the nuclear envelope (h and h′). pv, proacrosomal vesicles; g, Golgi; n, nucleus; ag, acrosomal granule; apx, acroplaxome. Photo credit: Aijie Xin, Fudan University.

male mice for fertility assessment. Consistent with the findings in the two affected brothers, spermatozoa from the *Actl7a*$^{KI/KI}$ mice failed to fertilize normal mouse oocytes by IVF (fig. S5). After ICSI, the fertilization also failed (fig. S5), whereas human spermatozoa of the affected brothers could fertilize oocytes by ICSI but arrested at early embryo stage (fig. S2). This may be due to the evolutionary divergence of ACTL7A function between human and mouse.

The failure of fertilization by ICSI performed with the sperm from *Actl7a*$^{KI/KI}$ male mice may be mainly due to failed oocyte activation and lack of the sperm-borne activating factor (SOAF) [i.e., phospholipase Cζ (PLCζ)] located in perinuclear theca (PT) (*5*). To explore this possibility, we first measured the thickness of two regions of PT, the subacrosomal layer (SAL-PT) and the postacrosomal sheath (PAS-PT), in the sperm from both brothers and *Actl7a*-mutated mice. Obviously, the thickness of both SAL-PT and PAS-PT was significantly increased in affected sperm (fig. S6).

PLCζ is one of the essential proteins located in PT. The abnormal thickness of PT might cause changes of PLCζ. Therefore, we investigated the expression and distribution of PLCζ in the sperm from *ACTL7A/Actl7a*-mutated human and mice by Western blotting and immunofluorescence. As shown in Fig. 5A, both affected human and mouse sperm samples presented sharp decreases of PLCζ when compared with normal controls. The reduced amount of PLCζ was confirmed by immunofluorescence. The total signals of PLCζ demonstrated reduced intensity in the sperm from human individuals and mice carrying homozygous *ACTL7A/Actl7a* mutations (Fig. 5B). In addition, as previously shown, PLCζ is located in the acrosomal and equatorial region of sperm heads in normal men and WT mice (Fig. 5B) (*6*, *7*). However, PLCζ signals were only detected in the acrosomal region of *ACTL7A*-mutated sperm, but not in the equatorial region (Fig. 5B), which is the area that first fuses with the oocyte. Besides, with the change of acrosomal morphology, PLCζ changed from the sickle shape to the cap-like structure in the sperm from *Actl7a*$^{KI/KI}$ mice (Fig. 5B). Together, Western blotting and immunofluorescence studies in human and mouse sperm indicated that the homozygous *ACTL7A* mutation resulted in the reduced amount and altered distribution of PLCζ, which could be responsible for the fertilization and developmental failure observed in human and mouse oocytes/embryos.

AOA is an efficient method to restore fertilization because of abnormal PLCζ presence in sperm (*8*). Therefore, we attempted the AOA technique using strontium chloride ($SrCl_2$). AOA following ICSI rendered the sperms of *Actl7a*$^{KI/KI}$ mice capable of successfully fertilizing the oocytes, and the resultant embryos developed into blastulas in vitro (Fig. 5C and table S3). To further investigate whether AOA could enable the homozygous *Actl7a*-mutated male mice to have their own offspring, the two-cell embryos were transplanted into pseudo-pregnant mice. Encouragingly, the embryos were successfully implanted and developed into pups (Fig. 5D and fig. S7A). These offspring of the *Actl7a*$^{KI/KI}$ male mice could reproduce through natural mating, and their farrowing rates presented no significant difference when compared to the mice from the control group (fig. S7B). These results indicated that the *Actl7a*-associated male infertility could be successfully overcome by AOA following ICSI.

The efficiency of the AOA method provides a significant therapeutic promise for patients with infertility resulting from the *ACTL7A* mutation. Brother 2 in this study volunteered to try this method and signed the informed consent. After controlled ovarian hyperstimulation (COH), four matured MII oocytes were obtained from brother 2's wife. Encouragingly, the technique of AOA with $SrCl_2$ made three oocytes fertilized and generated two good-quality embryos on day 3 (Fig. 5E and movies S1 to S4). These two embryos were transferred into the uterus of brother 2's wife during the second menstrual cycle after COH. Unfortunately, 14 days after the

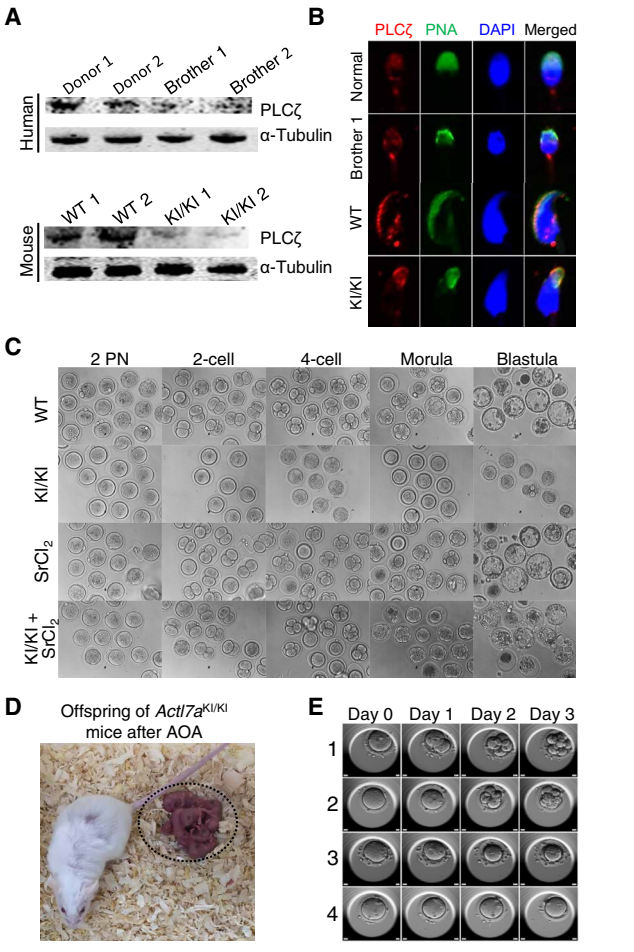

Fig. 5. Altered expression and distribution of PLCζ in the sperm from *ACTL7A/Actl7a*-mutated males and overcoming male infertility by AOA. (**A**) The PLCζ protein was significantly reduced in both human and mouse sperm affected by *ACTL7A/Actl7a* mutations. α-Tubulin was used as a loading control. (**B**) Confocal immunofluorescence images revealed the mislocalization of PLCζ on *ACTL7A/Actl7a*-mutated sperm. Single-sperm immunofluorescence analysis for PLCζ (red) and PNA (green) was performed in both human and mouse spermatozoa with *ACTL7A/Actl7a* mutations. Nuclei were stained with DAPI (blue). (**C**) The oocytes were fertilized by the sperms from the *Actl7a*-mutated male mice after AOA. ICSI failed to enable the sperms from the $Actl7a^{KI/KI}$ mice to fertilize the normal oocytes (lane 2). However, AOA using $SrCl_2$ rendered the sperms from $Actl7a^{KI/KI}$ mice capable of successfully fertilizing the oocytes, leading to the development of the resulting embryos into blastulas (lane 3). (**D**) Representative images of the offspring (dotted circle) of the $Actl7a^{KI/KI}$ male mice born after the combination of ICSI and AOA. (**E**) Representative images of the embryonic development from days 0 to 3 following ICSI with AOA in case of brother 2 and his wife. Numbers 1 to 4 represent the four matured MII oocytes acquired after subjecting the oocytes from brother 2's wife to COH. The development of the four embryos from days 0 to 3 is shown horizontally. Embryos 1 and 2 developed normally and were subsequently transplanted. Photo credit: Ronggui Qu, Fudan University.

transplantation, the implantation of the embryos failed. Brother 2's wife was 35 years old when this procedure was performed; this may be partially responsible for the failure of implantation. Nevertheless, AOA with $SrCl_2$ can overcome the *ACTL7A*-mutated sperm-derived embryonic arrest, promote the development of viable and transplantable embryos, and improve the embryo quality.

DISCUSSION

Early embryonic arrest has always been a challenge in assisted reproduction centers; the clinicians generally attribute the cause to the female factors, especially when sperm was "normal" by routine diagnosis of reproductive medicine. In this study, we found a previously unknown male factor responsible for the arrest of early embryonic development in humans and identified a homozygous mutation in *ACTL7A*, leading to male infertility by WES in a consanguineous family with two brothers. By the construction of a mouse model with the *Actl7a* knock-in mutation, we confirmed that the homozygous missense mutation of *Actl7a* could lead to acrosomal defects and reduced expression and abnormal distribution of PLCζ in sperms. AOA could successfully overcome the infertility of $Actl7a^{KI/KI}$ male mice, which is meaningful in the future practice of IVF/ICSI for the *ACTL7A*-mutated male infertility in humans.

Semen analyses, including the assessment of sperm concentration, motility, and morphology, of both the brothers by the regular diagnosis of reproductive medicine revealed normal. However, after the ultrastructural observation by TEM, the sperm acrosome is significantly disrupted, which cannot be revealed under light microscopy used for clinical laboratory tests. Therefore, such male cases will be false negative for clinical semen tests and incorrectly diagnosed as "normal" males. The previously unidentified homozygous *ACTL7A* mutation identified in a consanguineous family with two infertile brothers and the recapitulate phenotypes in *Actl7a* knock-in mouse model provide a convenient way for clinical diagnosis. The genetic test of *ACTL7A* mutation can be an efficient method to identify this previously neglected male factor for the early embryonic arrest, which will be informative for improving clinical practice of IVF/ICSI and help clinical doctor investigate the etiology of infertility and diagnose complex cases of infertility.

The acrosome is a unique membranous organelle containing a number of hydrolytic enzymes; it plays important roles in the penetration of the egg's zona pellucida and in the interaction between the plasma membranes of the sperm and the egg. Acrosomal integrity is critical to fertilization. Acrosomal defects have been reported to cause male infertility in humans (*9*, *10*). Ruffled acrosomes are associated with subfertility (*11*). The ruffling of acrosomes because of homozygous *ACTL7A* mutations may lead to the failure of the penetration of the egg's coats by sperms. Sperm acrosomal defects could be one of the major reasons for unsuccessful fertilization during IVF treatment in humans and mice.

Acrosome biogenesis involves the transport and fusion of Golgi-derived proacrosomal vesicles along the acroplaxome. It is known that the acroplaxome is a cytoskeletal plate that plays important roles in stabilizing the acrosome during acrosome biogenesis and anchoring the acrosome to the nuclear envelope during the shaping of the sperm head (*12*, *13*). It has been reported that ACTL7A is testis-specific and localized in acroplaxome (*3*). However, our ultrastructural assays in the sperm from $Actl7a^{KI/KI}$ mice showed the normal structure of acroplaxome and the proacrosomal vesicles anchoring on the nuclear envelopes during Golgi and Cap phase. This experimental evidence suggests that ACTL7A does not prevent the development and function of the acroplaxome. During early spermiogenesis, the Golgi apparatus secretes numerous small proacrosomal vesicles that gradually accumulate, coalesce, and migrate into the apical cytoplasm. Our TEM observation revealed that the Golgi apparatus generated big and atypical proacrosomic vesicles during Golgi phase, and they failed to fuse with the acrosome and

gradually accumulate, coalesce, and eventually cause the acrosome detached from the nuclear envelope.

Perinuclear matrix, also called PT, harbors proteins essential for spermiogenesis and fertilization. PLCZ1 or PLCζ is a well-recognized SOAF and located in the PT facing the acrosome and equatorial region (*6*, *7*, *14*–*16*). Changes in the expression or position of PLCζ are associated with subfertility or even infertility owing to the unsuccessful initiation of embryonic development (*15*, *17*–*19*). It is reported that sperm with absent or abnormal acrosome showed absence or lower amount of PLCζ and failed to fertilize oocytes (*6*, *20*). In sperm from both affected bothers and *Actl7a*-mutated male mice, the PT thickness was remarkably increased, and PLCζ presented lower amount and its signal located in the equatorial region disappeared, which is the region that first fuses with the oocyte and released SOAF into the oocyte for activation. This strongly suggested that the homozygous *ACTL7A* mutation caused acrosomal defects, which were associated with PT disruption and resulted in the reduced amount and abnormal localization of PLCζ. This was potentially responsible for the *ACTL7A*-associated fertilization and developmental failure observed in human and mouse oocytes/embryos.

We found that the homozygous *Actl7a* mutation caused the failure of oocyte activation in mice, but the arrest of embryonic development in humans. It has been reported that the duration of oocyte activation, patterns of calcium oscillations, and calcium channel blockers affect the early embryonic development in mice (*14*, *21*, *22*). In addition, sperms with low levels of PLCζ have been reported to be significantly related to higher rates of embryonic development arrest in humans (*23*). It is possible that trace amounts of PLCζ are not sufficient to completely initiate calcium oscillations, leading to the arrest of embryonic development. With the help of AOA with $SrCl_2$ in vitro, the embryos acquire sufficient and adequate calcium oscillations and eventually overcome the early embryonic developmental arrest.

$SrCl_2$ is a common chemical reagent for parthenogenetic activation of mouse oocytes. After activation, the mouse parthenogenetic embryos can develop to blastocysts but die by day 10 of gestation (*24*). In this study, AOA with $SrCl_2$ rendered the sperms of *Actl7a*$^{KI/KI}$ mice capable of successfully fertilizing the oocytes and the resultant embryos could develop into viable pups. Following genotyping, all the pups were heterozygotes, which suggested that they developed from zygotes resulting from the union of the mutant sperms and eggs rather than parthenogenetic embryos.

Currently, AOA is mainly being used to help individuals with recurrent fertilization failure, acephalic spermatozoa syndrome, and failure of fertilization after ICSI (*25*–*27*). Our investigation demonstrated that AOA may potentially be an effective method for ameliorating embryo development failure. However, further studies on a large number of male patients are required to investigate the correlations between the sperm ACTL7A levels, implantation rates, embryo development rates, and the clinical pregnancy rates.

Successful embryo implantation requires both good-quality embryos and appropriate maternal conditions. Age is a major factor influencing maternal fertility. Pregnancy rates have been reported to decease progressively with the increase in the age of females. The implantation rates during the ART cycles demonstrated a similar trend. It has been reported to be 41.3% in women younger than 35 years but decline to 21.0% in women aged 38 to 40 years (*28*, *29*). Age is the deciding factor in terms of the ovarian reserve. As the age of the female increases, the ovarian reserve decreases (*30*). Brother 2's wife was 39 years old when the ART cycle combined with AOA was performed; only four oocytes were acquired following COH. The age-related decrease of the ovarian reserve may be partly responsible for the failure of the implantation of the embryos in this case.

In summary, the homozygous mutation of *ACTL7A* first identified in a consanguineous family with two unexplained infertile brothers is responsible for early embryonic arrest and male infertility. The mutation leads to acrosomal defects and abnormal presence of PLCζ. Fortunately, AOA could successfully overcome embryonic arrest and make the *Actl7a* mutation mice have offspring. The genetic test based on our newly revealed knowledge of ACTL7A mutation can be an efficient method to identify this previously neglected male factor for the early embryonic arrest, which will be informative for improving clinical practice of IVF/ICSI. Our findings will facilitate genetic diagnoses and provide potential guidance to clinicians for appropriate therapeutic measures.

MATERIALS AND METHODS

Study subjects

The consanguineous family with two couples affected by unexplained infertility and the donors were recruited from the Shanghai Ji Ai Genetics and IVF Institute (Shanghai, China). All the included human studies were approved by the Ethics Committee of the Shanghai Ji Ai Genetics and IVF Institute (JIAI E 2018-21). Written informed consents were obtained from all the subjects participating in the study. All the human and animal subjects were performed according to a protocol approved by the Animal Care Committee of the Shanghai Institute of Planned Parenthood Research (2015-12) and conformed to the International Review Board and/or Institutional Animal Care and Use Committee guidelines.

Genetic and bioinformatic analyses

Genomic DNA was extracted from the peripheral blood leukocytes of the two brothers and their parents. Whole-exome capture and sequencing was performed using the Agilent SureSelect Whole Exome capture and Illumina sequencing technology following the standard procedures. The reads were aligned to the human genome reference assembly (hg19) with the Burrows-Wheeler Aligner. The candidate mutations met the following criteria: (i) the sharing by the two brothers and (ii) a low allele frequency in the public human genome databases of the 1000 Genomes Project and the gnomAD. The candidate mutation was validated using Sanger sequencing. Three predictors for deleterious variants, including PolyPhen-2, PROVEAN Protein Batch, and MutationTaster, were also used in this study.

Semen analysis and sperm preparation

In clinical practice, the semen parameters were analyzed according to the fifth edition of the WHO laboratory manual. After liquefication, the semen samples were evaluated for sperm concentration, total motility, viability, and round cell concentration under the light microscope. The normal semen should present 15×10^6/ml concentration, ≥40% total motility, ≥58% viability, and ≤1×10^6/ml round cell concentration. For assessment of sperm morphology, 20 μl of semen was spread over slides, dried at room temperature, and fixed in 95% ethanol for Papanicolaou stain. Spermatozoa were then assessed by ×100 oil-immersion bright-field objective according to the standard of the fifth edition of the WHO guidelines.

To prepare samples for laboratory experiments, the semen were separated using the SpermGrad gradient solution (Vitrolife, Sweden), using 90 and 45% discontinuous gradients. The sperms with good motility and morphology were collected from the lowest layer formed by the 90% gradient solution and washed using SpermRinse.

For the mouse studies, spermatozoa were released from the cauda epididymis into a modified human tubal fluid (HTF) medium (Millipore, USA), and their motility was analyzed by a computer-assisted sperm analysis program HTM-TOXIVOS (Hamilton-Thorn Research, MA). A small fraction of the washed sperm samples from the patients or mice was fixed with 4% paraformaldehyde (PFA) for 20 min, followed by two washes with phosphate-buffered saline (PBS) for the immunofluorescence analysis. The remaining fractions were aliquoted and stored at −80°C for Western blotting analysis.

Transmission electron microscopy

The washed human sperm and the mouse sperm from cauda epididymis were used for investigating sperm ultrastructures. The testes from WT and *Actl7a*$^{KI/KI}$ mice were used for studying acrosome biogenesis. All the samples were fixed with 2.5% glutaraldehyde for 24 hours at 4°C. The specimens were embedded in Epon 812 according to a standard TEM procedure and cut into ultrathin sections; they were then stained with uranyl acetate and lead citrate for subsequent observation and photography by TEM (Tecnai-10, Philips).

Generation of a knock-in mutant of mouse ortholog *Actl7a*

CRISPR-Cas9 technology was used to edit the mouse genome, as reported in a previous study (*31*). The target of single-guide RNAs and the single-stranded oligonucleotides (ssODNs) are shown in table S4. The guide RNA, Cas9 mRNA, and ssODNs were pooled and injected into the zygotes from C57BL/6 mice. The founder mice were crossed with WT C57BL/6 mice to obtain offspring. The genotyping primers used were as follows: 5′-GAGAAGTACGCCGAGATGCT-3′ (forward) and 5′-CTCCTGACCCAGACGGATCT-3′ (reverse). This study was performed in accordance with the recommendations of the *Guide for the Care and Use of Laboratory Animals* of the U.S. National Institutes of Health.

Fertility assessment of mice

The sexually mature male mice (8 to 12 weeks old) and female C57BL/6J mice (8 to 12 weeks old) were mated 1:2 to assess the fertility of the *Actl7a*-mutated male mice. The vaginal plugs of the mice were examined every morning. Then, the female mice with vaginal plugs were separately fed. The litter sizes were recorded after 21 days. If no pup was born within 22 days after sexual intercourse, the mice were subjected to laparotomy to confirm the result. The fertility of the offspring of the *Actl7a*$^{KI/KI}$ mice was assessed by the same method. The control mice were the offspring of the WT mice; they were born following ICSI.

Quantitative RT-PCR

The total RNA from the testis was extracted using the TRIzol reagent, according to the manufacturer's instructions. The complementary DNA (cDNA) templates were reverse-transcribed from the RNA samples using a reverse transcription PCR (RT-PCR) kit (TOYOBO, Japan). *Gapdh* served as the reference gene. The primers used were as follows: *Actl7a*, 5′-TCTCAACAACAGTGGGCAAG-3′ (forward) and 5′-CTGTGTCCCAGTCCACAATG-3′ (reverse); *Gapdh*, 5′-ACCCAGAAGACTGTGGATGG-3′ (forward) and 5′-TTCAGCTCAGGGATGACCTT-3′ (reverse). The amplification conditions were as follows: a denaturation step at 95°C for 10 min, followed by 40 cycles at 95°C for 10 s and 55°C for 30 s. The relative expression levels of the samples were quantified by the $2^{-\triangle Ct}$ method, where $^{\triangle}C_t = C_t$ (*Actl7a*) − C_t (*Gapdh*).

Protein extraction and Western blotting analysis

The proteins from the testes of adult mice were extracted using 1× radioimmunoprecipitation assay lysis buffer (Biotech Well, Shanghai, China) containing 1 mM phenylmethylsulfonyl fluoride and protease inhibitor cocktail (Biotech Well) on ice. The supernatants were collected following centrifugation (16,000*g* for 20 min) and stored at −80°C after appropriate aliquoting. The proteins from the sperms were extracted by boiling the samples for 5 min in 2% SDS buffer. Then, the samples were centrifuged at 16,000*g* for 20 min at room temperature. The supernatants were collected for subsequent Western blotting analysis.

The protein samples were separated by 12% SDS–polyacrylamide gel electrophoresis; the resulting bands were transferred onto polyvinylidene fluoride membranes (GE Healthcare, WI, USA) by the semidry method. The membranes were blocked for 2 hours with 5% nonfat milk in TBS buffer (containing 10 mM tris-HCl and 150 mM NaCl) and incubated with primary rabbit polyclonal antibodies against ACTL7A (1:1000; HPA021624, Atlas Antibodies) and PLCζ (for human sperm: 10 μg/ml, pab0367-P, Covalab; for mouse sperm: 1:400, ab124446, Abcam) overnight at 4°C and then with the horseradish peroxidase–labeled secondary antibodies (1:10,000; CWBiotech, Beijing, China) for 1 hour at room temperature. Next, the membranes were washed thoroughly with TBST buffer [20 mM tris-HCl, 150 mM NaCl, and 0.05% (v/v) Tween 20], and the bands were detected using an ECL kit (GE Amersham, Pittsburgh, USA). The semiquantification of the target protein and reference protein levels was performed using the ImageJ 1.48 grayscale scanning software.

Histological analysis and immunofluorescence

For the histological analysis, the fresh testis samples and different segments of the epididymis were fixed with 4% PFA overnight at 4°C and then embedded in paraffin. The paraffin-embedded specimens were cut into 4-μm-thick sections, followed by dewaxing, benzene removal, and hydration. Then, the prepared slices were stained with hematoxylin and eosin. Images were recorded using an Olympus BX60 microscope.

For immunofluorescence staining, the washed sperm samples were fixed with 4% PFA for 20 min, followed by two washes with PBS, and smeared onto polylysine-coated slides. After drying, sperm samples were permeabilized with PBS containing 0.3% Tween 20 and 0.2% Triton X-100 for 30 min. Next, they were washed thrice with PBS and blocked with 30% donkey serum containing 2% bovine serum albumin for 1 hour at room temperature. The slides were then incubated with rabbit polyclonal antibodies against ACTL7A (1:200, HPA021624, Atlas Antibodies), acrosin (1:100, NBP2-14260, Novus Biologicals), or PLCζ (for human sperm: 10 μg/ml, pab0367-P, Covalab; for mouse sperm: 1:100, ab124446, Abcam) overnight at 4°C. After being washed thrice with PBST (containing 0.05% Tween 20), the slides were incubated with donkey anti-rabbit immunoglobulin G (IgG) conjugated with Cy3 (1:500; Invitrogen, USA) for 1 hour at room temperature. The slides were then incubated with Alexa Fluor 488–conjugated PNA (20 μg/ml; Molecular Probes, CA, USA) for detecting the sperm acrosomes. The negative

control used was rabbit IgG. Last, the sections were mounted with one drop of DAPI (4′,6-diamidino-2-phenylindole) Fluoromount-G (SouthernBiotech, Birmingham, AL, USA) for image acquisition using the Nikon A1 + Confocal Microscope System (Tokyo, Japan).

IVF and ICSI in mice

B6D2F1 female mice (6 to 8 weeks old) were used as mature oocyte donors. Superovulation was performed by the intraperitoneal injection of 10 IU of pregnant mare serum gonadotropin (Ningbo Second Hormone Factory, China); 48 hours later, 10 IU of human chorionic gonadotropin (hCG; Livzon, China) was injected into the mice. The cumulus-oocyte complexes (COCs) were obtained by dissecting the ampulla at 13 to 15 hours after hCG injection.

Spermatozoa were released from the cauda epididymis into modified HTF medium (Millipore, USA) and screened by the swim-up method. For IVF, 5 to 10 μl of the sperm suspension were added to the COCs in a fertilization dish. After 6 hours, the eggs were washed several times to remove the cumulus cells and excess spermatozoa and then transferred into a new culture dish with KSOM medium. For ICSI, the spermatozoa were subjected to sonication for obtaining the spermatic heads. MII oocytes were collected by removing the cumulus cells through the digestion of the COCs with hyaluronidase (100 IU/ml) in M2 medium (Sigma-Aldrich, St. Louis, USA). The naked oocytes were washed three to four times in KSOM medium (Millipore, MA, USA) and cultured at 37°C under 5% CO_2 conditions for ICSI micromanipulation. Single sperm heads were injected into the oocytes of WT mice using a micromanipulator, with the Piezo apparatus (Eppendorf, Hamburg, Germany). These oocytes were then transferred into the KSOM medium, which was overlaid with mineral oil, after 15 min, and cultured at 37°C under conditions of 5% CO_2 and 95% humidity. The embryonic development was analyzed in the following days, and the two-cell zygotes were transferred into the oviducts of pseudo-pregnant ICR female mice that had been mated with vasectomized males during the previous night. The pups were obtained via natural labor.

Ovarian stimulation and ICSI in humans

Women were subjected to ICSI treatment in the center as clinically indicated. Ovarian stimulation was performed using the mild stimulation protocol with CC (Clomiphene Citrate Tablets, Codal Synto Ltd., Limassol, Cyprus) in combination with hMG (Menotrophins for Injection, Lizhu Pharmaceutical, China). Oocyte retrieval was performed 34 to 35 hours after the triggering step with hCG. The cumulus cells were removed before ICSI. Fertilization and embryonic development were monitored using time-lapse monitoring. All the media used for ICSI and embryo culture were purchased from Vitrolife (Gothenburg, Sweden, G5 series plus).

Assisted oocyte activation

The oocytes from mice were exposed to 5 mM $SrCl_2$ (Sigma-Aldrich, St Louis, MO, USA) in KOSM medium for 6 hours after ICSI. Following AOA, the oocytes were rinsed twice in KOSM medium and further cultured in the same medium at 37°C under conditions of 5% CO_2 and 95% humidity.

In humans, the medium for activation was first prepared; 1 ml of G1 medium supplemented with 5 mM EGTA (for chelating Ca^{2+}) was equilibrated in an incubator for at least 2 hours. Then, 10 mM $SrCl_2$ was added to this solution before ICSI. The oocytes were incubated in G-MOPS at 37°C and 5% CO_2 conditions for 30 min after ICSI and then transferred into the prepared activation buffer for 4 hours. Following AOA, the oocytes were subsequently rinsed several times in G1 medium and then cultured in accordance with the routine embryo culture procedure.

Statistical analyses

All data were presented as means ± SEM. Statistical analysis was performed using Prism GraphPad 5 software by means of the two-tailed Student's *t* test or one-way analysis of variance (ANOVA). *P* values of less than 0.05 were considered statistically significant.

SUPPLEMENTARY MATERIALS

Supplementary material for this article is available at http://advances.sciencemag.org/cgi/content/full/6/35/eaaz4796/DC1

View/request a protocol for this paper from *Bio-protocol*.

REFERENCES AND NOTES

1. A. M. Alazami, S. M. Awad, S. Coskun, S. Al-Hassan, H. Hijazi, F. M. Abdulwahab, C. Poizat, F. S. Alkuraya, *TLE6* mutation causes the earliest known human embryonic lethality. *Genome Biol.* **5**, 240 (2015).
2. Q. Sang, B. Li, Y. Kuang, X. Wang, Z. Zhang, B. Chen, L. Wu, Q. Lyu, Y. Fu, Z. Yan, X. Mao, Y. Xu, J. Mu, Q. Li, L. Jin, L. He, L. Wang, Homozygous mutations in *WEE2* cause fertilization failure and female infertility. *Am. J. Hum. Genet.* **102**, 649–657 (2018).
3. B. Boëda, P. P. Knowles, D. C. Briggs, J. Murray-Rust, E. Soriano, B. K. Garvalov, N. Q. McDonald, M. Way, Molecular recognition of the Tes LIM2–3 domains by the actin-related protein Arp7A. *J. Biol. Chem.* **286**, 11543–11554 (2011).
4. H. Yaguchi, N. Ohkura, M. Takahashi, Y. Nagamura, I. Kitabayashi, T. Tsukada, Menin missense mutants associated with multiple endocrine neoplasia type 1 are rapidly degraded via the ubiquitin-proteasome pathway. *Mol. Cell. Biol.* **24**, 6569–6580 (2004).
5. M. Javed, N. Esfandiari, R. F. Casper, Failed fertilization after clinical intracytoplasmic sperm injection. *Reprod. Biomed. Online* **20**, 56–67 (2010).
6. J. Escoffier, S. Yassine, H. C. Lee, G. Martinez, J. Delaroche, C. Coutton, T. Karaouzène, R. Zouari, C. Metzler-Guillemain, K. Pernet-Gallay, S. Hennebicq, P. F. Ray, R. Fissore, C. Arnoult, Subcellular localization of phospholipase Cζ in human sperm and its absence in DPY19L2-deficient sperm are consistent with its role in oocyte activation. *Mol. Hum. Reprod.* **21**, 157–168 (2015).
7. A. Ferrer-Vaquer, M. Barragan, T. Freour, V. Vernaeve, R. Vassena, PLCζ sequence, protein levels, and distribution in human sperm do not correlate with semen characteristics and fertilization rates after ICSI. *J. Assist. Reprod. Genet.* **33**, 747–756 (2016).
8. E. Heytens, T. Schmitt-John, J. M. Moser, N. M. Jensen, R. Soleimani, C. Young, K. Coward, J. Parrington, P. De Sutter, Reduced fertilization after ICSI and abnormal phospholipase C zeta presence in spermatozoa from the wobbler mouse. *Reprod. Biomed. Online* **21**, 742–749 (2010).
9. E. Moretti, G. Collodel, G. Scapigliati, I. Cosci, B. Sartini, B. Baccetti, 'Round head' sperm defect. Ultrastructural and meiotic segregation study. *J. Submicrosc. Cytol. Pathol.* **37**, 297–303 (2005).
10. R. J. Aitken, L. Kerr, V. Bolton, T. Hargreave, Analysis of sperm function in globozoospermia: Implications for the mechanism of sperm-zona interaction. *Fertil. Steril.* **54**, 701–707 (1990).
11. P. J. Chenoweth, Genetic sperm defects. *Theriogenology* **64**, 457–468 (2005).
12. A. L. Kierszenbaum, E. Rivkin, L. L. Tres, Acroplaxome, an F-actin–keratin-containing plate, anchors the acrosome to the nucleus during shaping of the spermatid head. *Mol. Biol. Cell* **14**, 4628–4640 (2003).
13. A. L. Kierszenbaum, E. Rivkin, L. L. Tres, Molecular biology of sperm head shaping. *Soc. Reprod. Fertil. Suppl.* **65**, 33–43 (2007).
14. C. M. Saunders, M. G. Larman, J. Parrington, L. J. Cox, J. Royse, L. M. Blayney, K. Swann, F. A. Lai, PLCζ: A sperm-specific trigger of Ca^{2+} oscillations in eggs and embryo development. *Development* **129**, 3533–3544 (2002).
15. S.-Y. Yoon, T. Jellerette, A. M. Salicioni, H. C. Lee, M.-S. Yoo, K. Coward, J. Parrington, D. Grow, J. B. Cibelli, P. E. Visconti, J. Mager, R. A. Fissore, Human sperm devoid of PLC, zeta 1 fail to induce Ca^{2+} release and are unable to initiate the first step of embryo development. *J. Clin. Invest.* **118**, 3671–3681 (2008).
16. S. Fujimoto, N. Yoshida, T. Fukui, M. Amanai, T. Isobe, C. Itagaki, T. Izumi, A. C. Perry, Mammalian phospholipase Czeta induces oocyte activation from the sperm perinuclear matrix. *Dev. Biol.* **274**, 370–383 (2004).
17. E. Heytens, J. Parrington, K. Coward, C. Young, S. Lambrecht, S.-Y. Yoon, R. A. Fissore, R. Hamer, C. M. Deane, M. Ruas, P. Grasa, R. Soleimani, C. A. Cuvelier, J. Gerris, M. Dhont,

D. Deforce, L. Leybaert, P. De Sutter, Reduced amounts and abnormal forms of phospholipase C zeta (PLCζ) in spermatozoa from infertile men. *Hum. Reprod.* **24**, 2417–2428 (2009).
18. S. L. Taylor, S.-Y. Yoon, M. S. Morshedi, D. R. Lacey, T. Jellerette, R. A. Fissore, S. Oehninger, Complete globozoospermia associated with PLCζ deficiency treated with calcium ionophore and ICSI results in pregnancy. *Reprod. Biomed. Online* **20**, 559–564 (2010).
19. S. N. Amdani, C. Jones, K. Coward, Phospholipase C zeta (PLCζ): Oocyte activation and clinical links to male factor infertility. *Adv. Biol. Regul.* **53**, 292–308 (2013).
20. J. Escoffier, H. C. Lee, S. Yassine, R. Zouari, G. Martinez, T. Karaouzène, C. Coutton, Z.-e. Kherraf, L. Halouani, C. Triki, S. Nef, N. Thierry-Mieg, S. N. Savinov, R. Fissore, P. F. Ray, C. Arnoult, Homozygous mutation of PLCZ1 leads to defective human oocyte activation and infertility that is not rescued by the WW-binding protein PAWP. *Hum. Mol. Genet.* **25**, 878–891 (2016).
21. J.-P. Ozil, S. Markoulaki, S. Toth, S. Matson, B. Banrezes, J. G. Knott, R. M. Schultz, D. Huneau, T. Ducibella, Egg activation events are regulated by the duration of a sustained $[Ca^{2+}]_{cyt}$ signal in the mouse. *Dev. Biol.* **282**, 39–54 (2005).
22. G.-F. He, L.-L. Yang, S.-M. Luo, J.-Y. Ma, Z.-J. Ge, W. Shen, S. Yin, Q.-Y. Sun, The role of L-type calcium channels in mouse oocyte maturation, activation and early embryonic development. *Theriogenology* **102**, 67–74 (2017).
23. M. Aarabi, H. Balakier, S. Bashar, S. I. Moskovtsev, P. Sutovsky, C. L. Librach, R. Oko, Sperm content of postacrosomal WW binding protein is related to fertilization outcomes in patients undergoing assisted reproductive technology. *Fertil. Steril.* **102**, 440–447 (2014).
24. M. A. Surani, S. C. Barton, Development of gynogenetic eggs in the mouse: Implications for parthenogenetic embryos. *Science* **222**, 1034–1036 (1983).
25. S. T. Kim, Y. B. Cha, J. M. Park, M. C. Gye, Successful pregnancy and delivery from frozen-thawed embryos after intracytoplasmic sperm injection using round-headed spermatozoa and assisted oocyte activation in a globozoospermic patient with mosaic Down syndrome. *Fertil. Steril.* **75**, 445–447 (2001).
26. K. Nakagawa, S. Yamano, N. Moride, M. Yamashita, M. Yoshizawa, T. Aono, Effect of activation with Ca ionophore A23187 and puromycin on the development of human oocytes that failed to fertilize after intracytoplasmic sperm injection. *Fertil. Steril.* **76**, 148–152 (2001).
27. B. Heindryckx, J. Van der Elst, P. De Sutter, M. Dhont, Treatment option for sperm- or oocyte-related fertilization failure: Assisted oocyte activation following diagnostic heterologous ICSI. *Hum. Reprod.* **20**, 2237–2241 (2005).
28. American College of Obstetricians and Gynecologists Committee on Gynecologic Practice and Practice Committee, Female age-related fertility decline. Committee Opinion No. 589. *Fertil. Steril.* **101**, 633–634 (2014).
29. Centers for Disease Control and Prevention, American Society for Reproductive Medicine, Society for Assisted Reproductive Technology, *2015 Assisted Reproductive Technology National Summary Report* (U.S. Department of Health and Human Services, 2017).
30. W. H. Wallace, T. W. Kelsey, Human ovarian reserve from conception to the menopause. *PLOS ONE* **5**, e8772 (2010).
31. R. J. Platt, S. Chen, Y. Zhou, M. J. Yim, L. Swiech, H. R. Kempton, J. E. Dahlman, O. Parnas, T. M. Eisenhaure, M. Jovanovic, D. B. Graham, S. Jhunjhunwala, M. Heidenreich, R. J. Xavier, R. Langer, D. G. Anderson, N. Hacohen, A. Regev, G. Feng, P. A. Sharp, F. Zhang, CRISPR-Cas9 knockin mice for genome editing and cancer modeling. *Cell* **159**, 440–455 (2014).

Acknowledgments: We thank D. Li for comments on the manuscript. **Funding:** This work was supported by the Foundation of Science and Technology Commission of Shanghai Municipality (17JC1400902 and 17JC1420103), the National Natural Science Foundation of China (81401252, 81270744, 31625015, and 31521003), the Foundation of Shanghai Municipal Commission of Health and Family Planning (20164Y0157 and 20174Y0214), China Postdoctoral Science Foundation (2019 M661580), Shanghai Medical Center of Key Programs for Female Reproductive Diseases (2017ZZ01016), Science and Technology Major Project of Inner Mongolia Autonomous Region of China (zdzx2018065), and Shanghai Municipal Science and Technology Major Project (2017SHZDZX01). **Author contributions:** X.S., F.Z., and H.S. conceived and designed the experiments. A.X., R.Q., G.C., and L.Z. performed the experiments and drafted the manuscript. J.C., J.F., Y.C., and X.P. provided clinical samples and collected data. C.T. performed genotyping. J.T. and Y.R. analyzed data and provided ICSI technical assistance. All authors revised and approved the final manuscript. **Competing interests:** The authors declare that they have no competing interests. **Data and materials availability:** All data needed to evaluate the conclusions in the paper are present in the paper and/or the Supplementary Materials. Additional data related to this paper may be requested from the authors.

Submitted 24 September 2019
Accepted 15 July 2020
Published 28 August 2020
10.1126/sciadv.aaz4796

Citation: A. Xin, R. Qu, G. Chen, L. Zhang, J. Chen, C. Tao, J. Fu, J. Tang, Y. Ru, Y. Chen, X. Peng, H. Shi, F. Zhang, X. Sun, Disruption in *ACTL7A* causes acrosomal ultrastructural defects in human and mouse sperm as a novel male factor inducing early embryonic arrest. *Sci. Adv.* **6**, eaaz4796 (2020).